Articles

Micellar Bolaform and ω-Carboxylate Phosphatidylcholines as Substrates for Phospholipases†

Karen A. Lewis, Christine E. Soltys, Karmine Yu, and Mary F. Roberts*

Merkert Chemistry Center, Boston College, Chestnut Hill, Massachusetts 02167

Received December 13, 1993®

ABSTRACT: A series of mixed-chain diacyl-PCs which contain an ω-COOH on the *sn*-2 chain [1-C_x-2-C_y-(COOH)-PC] and bolaform (1-C_x-2,2′-C_y-1′-C_x-PC) phosphatidylcholines were synthesized and examined as substrates for phospholipase A_2 (*Naja naja naja*) and C (*Bacillus cereus*). There is very little detectable phospholipase A_2 activity toward pure micellar 1-acyl-2-acyl-(ω-COOH) species. In addition, when these same ω-COOH species are present at concentrations above their CMCs, they are potent inhibitors of phospholipase A_2 hydrolysis of other micellar lipids. In contrast, phospholipase C hydrolysis of the same 1-acyl-2-acyl-ω-COOH)-PC species proceeds with rates comparable to that of diheptanoyl-PC. The bolaform lipids, which are tethered through a common *sn*-2 acyl chain, (e.g., 1-C_8-2,2′-C_{12}-1′-C_8-PC) display quite different kinetic results. Under limiting Ca^{2+} conditions (100 μM) all the available *sn*-2 acyl bonds of the dimer are hydrolyzed. However, at high Ca^{2+} concentrations (1–10 mM) the reaction curves have a biphasic nature, characterized by an initial burst of activity followed by much slower rate. This is consistent with only the micellar 1-acyl-2-acyl-(ω-COOH)-PC produced *in situ* from phospholipase A_2 hydrolysis of the dimer acting as an inhibitor of subsequent phospholipase A_2 activity. Phospholipase C hydrolysis of the PC dimer and the *sn*-2 ω-COOH PC is rapid, with both available glycerophosphate groups cleaved at presumably the same rate. These results are discussed in terms of the unique physical properties (as measured by NMR and fluorescence experiments) of these phospholipids.

Current models of water-soluble phospholipases (Berg et al., 1992; Jain et al., 1989; Burack et al., 1993) suggest that two key steps are involved in catalysis: an initial binding to the substrate surface and then either a conformational change or a subsequent binding step which leads to catalysis. From this point the catalysis can be processive on the surface or can occur via diffusion of the enzyme from one substrate aggregate to another. For phospholipase A_2, negatively charged substrates appear to favor tight binding of the enzyme to the substrate surface (Berg et al., 1991; Ghomashchi et al., 1991a,b; Jain et al., 1991a–c]. There has also been the proposal that two phospholipids are required for activity (the "dual phospholipid" model) (Dennis & Pluckthun, 1986). That model suggests that there are two functionally distinct sites of the enzyme: a catalytic site, nonspecific for headgroup but requiring two fatty acyl chains, and an activator site, which is exclusive for a phosphocholine headgroup (Adamich et al., 1979; Roberts et al., 1979). Concrete information on phospholipid binding to the active site has been provided by the crystal structure of phospholipase A_2 with a bound transition state analogue where it appears that 6–8 carbons of the fatty acyl chains fill up the active site (Scott et al., 1990; White et al., 1990). The implication for interfacial activity is that removal of the phospholipid from the aggregate into the hydrophobic cavity of the enzyme is energetically the driving force for the enhanced rates observed toward micellar versus monomeric substrates.

Testing these different ideas can help to fine tune the mechanistic details of these enzymes and help generate specific inhibitors. Bolaform PCs are synthetic lipid species which possess two PC headgroups in the same molecule. They share three distinct hydrocarbon chains between the two glycerol moieties. These can be used to explore several of the mechanistic proposals mentioned above. "Dimeric" molecules with long-chain fatty acyl linkages joined through terminal acetylenic linkages have been synthesized previously (Hebert et al., 1992). The chain linkages in those molecules have rigid segments which could alter PC conformation and bilayer properties, and through these alter the binding of substrate to phospholipases. As an alternative to these species, a bolaform short-chain PC with a polymethylene chain that connects the *sn*-2 chains of two lyso-PCs has been synthesized. With a bolaform that forms micelles, kinetic complications from bilayer phase changes can be avoided. The bolaform PC molecules synthesized in the present work are tethered through a common *sn*-2 acyl chain (i.e., 1-C_8-2,2′-C_{12}-1′-C_8-PC). The result of one phospholipase A_2 catalytic event on a bolaform PC molecule generates the corresponding 1-acyl-2-acyl-(ω-COOH)-PC molecule (see Figure 1). This asymmetric PC with a terminal carboxylate in the *sn*-2 chain has been synthesized independently, physically characterized, and assayed as a substrate for phospholipases A_2 and C. These bipolar lipid species are especially interesting since the terminal carboxylate may be protonated or ionized, depending on the sample pH. This will be shown to modulate aggregate structure. The susceptibilities of the bolaform and 1-acyl-2-acyl-(ω-COOH)-PC species to phospholipases A_2 and C are interpreted in light of their physical properties and with respect to two-state lipid binding in micelles.

† This work was supported by NIH GM 26762.

* To whom correspondence should be addressed.

® Abstract published in *Advance ACS Abstracts,* April 1, 1994.

0006-2960/94/0433-5000$04.50/0

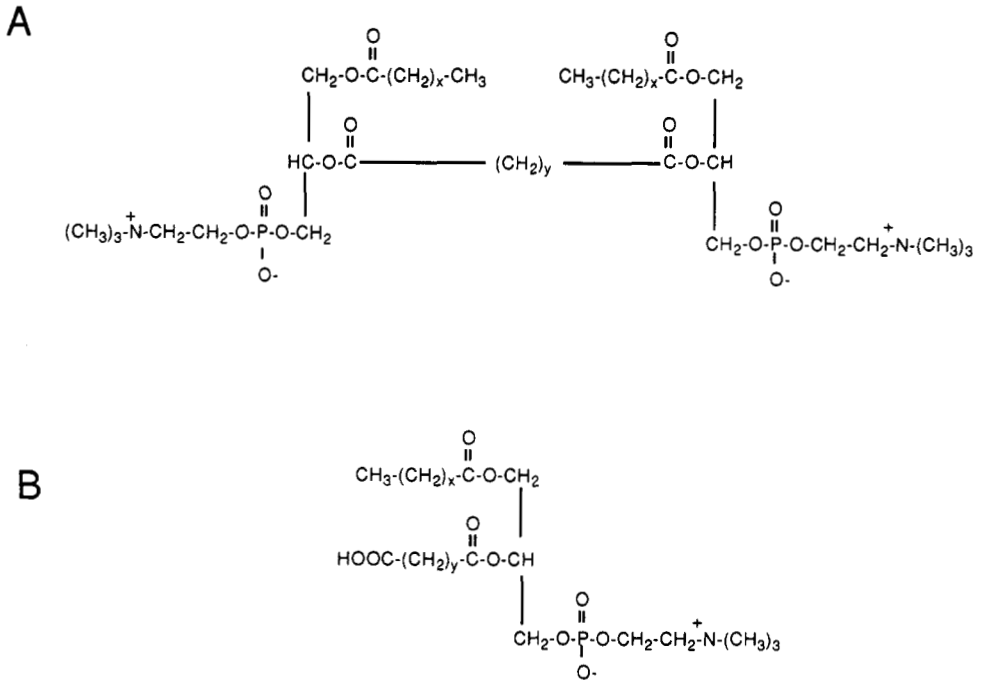

FIGURE 1: Structures of (A) short-chain bolaform or dimeric PCs and (B) 1-acyl-2-acyl-(ω-COOH)-PCs.

MATERIALS AND METHODS

Chemicals. 1-Octanoyl-PC, 1-hexanoyl-PC, and diheptanoyl-PC were purchased from Avanti Polar Lipids Inc. 1,10-Decanedicarboxylic acid, 1,12-dodecanedicarboxylic acid, and hexadecanedioic acid were obtained from Aldrich Chemical Co. in 98% or better purity. 1-C_8-2-C_4pyr-PC was synthesized from 1-octanoyl-PC and the corresponding pyrene fatty acid using 1,1′-carbonyl diimidazole (Aldrich) as described previously for the synthesis of 1-C_6-2-C_4pyr-PC (Soltys et al., 1993). Phospholipase A_2 (*Naja naja naja*) and phospholipase C (*Bacillus cereus*) were obtained from Sigma and used without further purification. MES buffer was purchased from Calbiochem-Behring Corp. Tris-HCl was obtained from Bethesda Research Labs.

Synthesis of Bolaform PCs. 1-C_8-2,2′-C_{12}-1′-C_8-PC was synthesized from 1-octanoyl-PC and 1,10-decanedicarboxylic acid by the fatty acid imidazole method (Burns et al., 1980, 1983) with the ratio of starting materials, dicarboxylic acid/1,1′-carbonyldiimidazole/1-octanoyl-PC, altered to 1:2.5:5. 1-C_6-2,2′-C_{16}-1′-C_6-PC was synthesized by the same modified method from 1-hexanoyl-PC and hexadecanedioic acid, respectively. Reaction progress was monitored by thin layer chromatography with a solvent system of $CHCl_3/CH_3OH/H_2O$ (62:32:6) and detection by iodine vapor staining. Bolaform PCs were purified by two successive silica gel columns and eluted with an increasing gradient of $CHCl_3/CH_3OH$. Preparative TLC was also performed to separate residual 1-acyl-2-acyl-(ω-COOH)-PC from bolaform PC [R_f bolaform = 0.30, R_f 1-acyl-2-acyl-(ω-COOH)-PC = 0.21]. Samples were loaded on glass-backed precoated silica gel plates (EM Laboratories, Inc.) followed by elution with $CHCl_3/CH_3OH/H_2O$ (62:32:6). 1-Acyl-2-acyl-(ω-COOH)-PC (a side product) and bolaform PCs were visualized by protecting the center of the plate with plastic wrap and exposing the edges to I_2 vapor. The silica resin containing the bolaform PC was scraped from the plate, mixed with the elution solvents, gently vortexed, bath sonicated, and then centrifuged for 10 min at 90*g* to sediment the silica gel. The supernatant was removed, concentrated by rotary evaporation, lyophilized, and subjected to a final silica gel column as described above.

^{13}C NMR resonances are diagnostic for backbone, headgroup, and acyl chain structural confirmation (Burns et al., 1980). Since both halves of the bolaform molecule are chemically equivalent, the ^{13}C spectrum of 1-C_x-2,2′-C_y-1′-C_x-PC[1] is characterized by two carbonyl resonances, two α-CH_2's (adjacent to the carbonyls), and other acyl chain carbons whose integrated intensities resemble 1-C_x-2-$C_{y/2}$-PC (Lewis et al., 1990). The only exception is the CH_3 resonance on the *sn*-1 chains which has half the intensity expected. These spectral characteristics were coupled with TLC assays to assess the presence or absence of contaminants. ^{13}C chemical shifts for the backbone and headgroup of 1-C_8-2,2′-C_{12}-1′-C_8-PC in CD_3OD (ppm from TMS) were as follows: 70.93 (CHO); 64.14 (glycerol CH_2OP); 62.80 (glycerol CH_2O); 66.59 (CH_2N); 57.68 (choline CH_2OP); 52.84 [$N(CH_3)_3$]. The *sn*-1 octanoyl chain resonances included 34.00 (C2), 25.15 (C3), 29.55 (C4–C6), 22.82 (C7), and 13.58 (C8). The *sn*-2 1,10-decanedioyl chain resonances included 34.23 (C2 and C11), 25.15 (C3 and C10), 32.01 (C4 and C9), and 29.55 (C5–C8). Since the backbone and headgroup resonances are essentially invariant with chain length, only the acyl chain carbon chemical shifts will be given for other compounds. Furthermore, when several resonances contribute to the bulk methylene region, the chemical shift reported is for the center of this region. For 1-C_8-2,2′-C_{14}-1′-C_8-PC, the *sn*-1 chain resonances included 34.20 (C2), 25.08 (C3), 29.46 (C4–C6), 22.74 (C7), and 13.57 (C8). The *sn*-2 chain resonances included 34.20 (C2 and C13), 25.08 (C3 and C12), 31.92 (C4 and C10), and 29.46 (C5–C9). For 1-C_6-2,2′-C_{16}-1′-C_6-PC, the *sn*-1 carbons included 34.01 (C2), 25.16 (C3), 29.56 (C4), 22.52 (C5), and 13.42 (C6). The *sn*-2 chain carbons included 34.23 (C2 and C15), 25.16 (C3 and C14), 31.53 (C4 and C13), and 29.56 (C5–C12).

Synthesis of 1-Acyl-2-acyl-(ω-COOH)-PCs. While a report of the synthesis of long-chain dialkylphospholipids containing a carboxyl group at the *sn*-1 chain terminus exists (Berchtold,

[1] Abbreviations: 1-C_x-2,2′-C_y-1′-C_x-PC, 1-acyl-2,2′-acyl-1-acyl-3-phosphocholine; 1-C_x-2-C_y-(ω-COOH)-PC, 1-acyl-2-acyl-(ω-COOH)-3-phosphocholines; CMC, critical micelle concentration; di-C_nPC, 1,2-diacyl-3-phosphocholine.

1981), such lipids have not been characterized in any physical detail. Furthermore, no short-chain diacyl-PCs with terminal carboxylates have been prepared and characterized. 1-C_8-2-C_{12}-(ω-COOH)-PC was synthesized from 1-octanoyl-PC and 1,10-decanedicarboxylic acid using carbonyldiimidazole in a ratio of 1:5:6. 1-C_8-2-C_{14}-(COOH)-PC and 1-C_6-2-C_{16}-(COOH)-PC were synthesized by the same method from 1-octanoyl-PC and 1,12-dodecanedicarboxylic acid or 1-hexanoyl-PC and hexadecanedioic acid, respectively. 1-Acyl-2-acyl-(ω-COOH)-PCs were purified by elution from two successive silica gel columns with an increasing gradient of $CHCl_3/CH_3OH$. These PCs were identified in the ^{13}C NMR spectrum by the presence of three carbonyl resonances (the most downfield one belonging to the ω-COOH), three CH_2's α to a carbonyl group, and an acyl chain pattern with more intensity in the bulk CH_2 region than the bolaform PCs. ^{13}C NMR chemical shifts for the backbone and headgroup of 1-acyl-2-acyl(ω-COOH)-PC species solubilized in CD_3OD were similar to the values observed for the bolaform PCs; only chain resonances differed significantly. For 1-C_8-2-C_{12}-(ω-COOH)-PC, *sn*-1 resonances included 34.00 (C2), 24.74 (C3), 29.01 (C4 and C5), 31.73 (C6), 22.56 (C7), and 13.84 (C8); *sn*-2 chain carbons included 34.03 (C2), 24.74 (C3), 29.01 (C4–C9), 25.63 (C10), 36.35 (C11), and 178.30 (C12). For 1-C_8-2-C_{14}-(ω-COOH)-PC, *sn*-1, resonances included 34.42 (C2), 24.51 (C3), 28.94 (C4 and C5), 31.38 (C6), 22.18 (C7), and 12.92 (C8); *sn*-2 chain carbons included 33.60 (C2), 24.51 (C3), 28.94 (C4–C11), 25.63 (C12), 36.09 (C13), and 180.15 (C14). For 1-C_6-2-C_{16}-(ω-COOH)-PC, *sn*-1 resonances included 34.00 (C2), 24.79 (C3), 29.55 (C4), 22.51 (C5), and 13.40 (C6); *sn*-2 chain carbons included 34.20 (C2), 25.12 (C3), 29.55 (C4–C13), 25.44 (C14), 34.64 (C15), and 177.50 (C16).

^{13}C NMR Spectroscopy. ^{13}C spectra were obtained in CD_3OD at 125.7 MHz on a Varian Unity 500 spectrometer. Significant spectral parameters include ^1H WALTZ decoupling, 25 000-Hz sweep width, 65 024 points, 6.0-μs (45°) pulse width, and 5000 transients per acquisition. Chemical shifts (ppm) were referenced to the central CD_3OD solvent peak at 49.0 ppm. ^{13}C NMR spin–lattice relaxation times (T_1) were measured in CD_3OD and D_2O using the inversion–recovery method (Vold et al., 1968). Spectral parameters were as described above with the exception of 12 τ values which ranged from 0.0375 to 19.2 s, 400–500 transients collected per τ value, and a recycle delay of 12 s between pulses. The 90° pulse was calibrated to be 12 μs. The error in the exponential analysis was typically <10%.

^{31}P NMR Spectroscopy. ^{31}P NMR (202.3 MHz) spectra of the 1-acyl-2-acyl-(ω-COOH)-PC samples in D_2O were obtained with the following parameters: 100 000 Hz sweep width, 128 000 points, 4.5-μs pulse, 2-s recycle delay and 64–2500 transients depending on the sample pH and aggregation state.

Critical Micelle Concentrations. Critical micelle concentrations were measured for each of the bolaform and 1-acyl-2-acyl-(ω-COOH)-PC species in pure water and additionally for some of the 1-acyl-2-acyl-(ω-COOH)-PC species in MES (pH 5) and Tris (pH 8) buffer to compare CMC values with the terminal carboxylate protonated or deprotonated. CMC values were determined by directly measuring the apparent surface tension (dynes/cm) for a series of PC concentrations with a Fisher Surface Tensiomat 21 utilizing the du Nouy ring method (Findlay, 1972). CMC values were determined for each of the PCs by the intersection of linear fits of the monomer and micellar regions of plots with surface tension vs the natural log of the lipid concentration. Colorimetric phosphate assays were performed on each sample to determine exact PC concentration (Chen et al. 1956; Turner & Rouser, 1970). Limiting surface areas were also determined from the data sets as previously described (Bian & Roberts, 1991, 1992).

pH-Stat Kinetic Analyses. Susceptibility of phospholipases A_2 and C toward the bolaform PCs and the 1-acyl-2-acyl-(ω-COOH)-PCs was quantified by titration of ionized product acid via the pH-stat method (Dennis, 1973). Conditions for assays (done at pH 8.0) were as previously described (Lewis et al., 1990). Varying amounts of Ca^{2+} (0.1–100 mM) were added to samples for phospholipase A_2 hydrolysis. The concentrations of stock solutions of phospholipases A_2 and C were determined by a colorimetric protein assay (Bradford, 1976). The quantity of phospholipase A_2 added typically ranged between 0.65 and 2 μg per assay while 1.2 μg or less of phospholipase C was usually added. Enzyme stock solutions were always adjusted to pH 8.0 prior to addition to assay solutions.

Quasielastic Light Scattering. The average hydrodynamic radius of different PC micelles was measured in a QLS system with a Brookhaven Instruments Digital Correlator BI-2030 AT with 72 channels and a 50-MW HE–NE laser as the light source (632.8 nm). Samples were filtered through a Millex-GV 0.22-μm filter (Millipore Corp.) into small (1-mL capacity) test tubes. Each sample was incubated ~5 min prior to data acquisition. The diffusion coefficient was extracted as the time constant in an exponential fit of the decay curve. An average hydrodynamic radius, R_H, was calculated from the measured diffusion coefficient, D, using the Stokes–Einstein relation ($D = kT/6\eta\pi R_H$), where T is the absolute temperature and η is the solvent viscosity.

Steady-State and Stopped-Flow Fluorescence Spectroscopy. Steady-state fluorescence measurements were made with a Shimadzu RF5000V spectrofluorimeter. To excite the short-chain pyrene-PC probe (1-C_8-2-C_4pyr-PC), the excitation wavelength was set at 352 nm, and the emission was monitored from 360 to 550 nm. Almost all the fluorescence information for both excimer and monomer bands was included in this range. The excitation bandwidth was 1.5–3 nm, and the emission bandwidth was 3 nm or larger. For monitoring the time scale of phospholipid mixing in micelles, a stopped-flow system was used.

Stopped-flow measurements of micelle mixing were made with a KinTek, Inc., stopped-flow spectrofluorimeter operating at 25 °C with a dead time of approximately 1 ms. Samples were excited at 350 nm with fluorescence detected (380 nm) directly by computer via a National Instruments analog/digital interface. One syringe contained the pyrene-labeled PC (1-C_8-2-C_4pyr-PC), while the second syringe contained the nonlabeled PC of interest. For each sample, at least five successive runs were made in order to ensure reproducibility of the observed rates.

RESULTS

Physical Characterization of Bolaform and 1-Acyl-2-acyl-(ω-COOH)-PCs. Table 1 lists the critical micellar concentrations (CMC), surface area per headgroup at the CMC (A_{CMC}), and hydrodynamnic radii (R_H) that were measured for the bolaform PCs and 1-acyl-2-acyl-(ω-COOH)-PCs. The concentrations for the bolaform species were expressed as $[P_i]/2$ since these molecules each possess two headgroups. 1-C_8-2-C_{12}-(ω-COOH)-PC was examined in H_2O, Tris buffer, and MES buffer to determine how the terminal carboxylate protonation state affected surface properties. The significantly

Table 1: Surface Properties of Bolaform and 1-Acyl-2-acyl-(ω-COOH)-PCs

lipid	buffer	CMC (mM)	A_{CMC} (Å²)[a]	R_H (Å)[b]
1-C_8-2,2′-C_{12}-1′-C_8-PC	H_2O	0.014[c]	42	800
1-C_6-2,2′-C_{16}-1′-C_6-PC	H_2O	<0.002[c]	–[d]	–
1-C_8-2-C_{12}-(ω-COOH)-PC	H_2O	1.0	65	780
1-C_8-2-C_{12}-(ω-COOH)-PC	MES, pH 6	1.5	94	640
1-C_8-2-C_{12}-(ω-COOH)-PC	Tris, pH 8	4.4	106	1800
1-C_8-2-C_{14}-(ω-COOH)-PC	H_2O	0.090	58	660
1-C_6-2-C_{16}-(ω-COOH)-PC	H_2O	0.022	80	410

[a] Area at the CMC for each phosphocholine moiety. [b] R_H (Å) values are reported for samples between 1.5 and 3 mM; polydispersities are typically 30–50%. [c] CMC for bolaform PCs is expressed per bolaform molecule rather than per phosphocholine headgroup. [d] Insufficient data at the lower concentrations to determine the area per phosphocholine headgroup accurately.

lower CMC for 1-C_8-2,2′-C_{12}-1′-C_8-PC than for di-C_7PC indicates that the shared polymethylene chain does not pack closely with the *sn*-1 acyl chain in the dimeric PC (Bian & Roberts, 1992). These dimeric PCs must pack into micelles to avoid H_2O contact with a substantial portion of the shared *sn*-2 polymethylene chain. For 1-C_8-2,2′-C_{12}-1′-C_8-PC, the area per phosphocholine moiety was measured to be 42.2 Å² (84.4 Å² per dimer), a value which is lower than that for diacyl-PCs, which are typically ~60–65 Å². For diacyl-PCs it has been proposed that the phosphocholine group dominates the surface area at the CMC. If the same is true for the bolaform PC, the observed area for the dimeric PC should be 120 Å² since there are two headgroups. If, in contrast, the close-packed chains determined the area/molecule, the surface area for the bolaform molecule would be expected to be 60–66 Å² (3 × 20–22 Å² per fatty acyl chain). If the shared *sn*-2 chain is not close packed, then the surface area for the bolaform molecule should be larger—this is consistent with the observed molecular area of 84 Å². This suggests that chain packing dominates the surface area for the bolaforms. These short-chain bolaform PC species form large micelles with R_H ~750–900 Å at 1–4 mM. A rod-shaped micelle consistent with this hydrodynamic radius would have >5000 molecules (Lin et al., 1987), and hence substrate depletion in a single micelle would not be a significant problem in the initial stages of the enzymatic hydrolysis reaction.

The CMC values measured for the 1-acyl-2-acyl-(ω-COOH)-PCs decreased with increasing numbers of methylenes present in the *sn*-2 (ω-COOH) acyl chain for each member in this series of compounds (Table 1). The CMC values measured in water for this series ranged from 22 μM for 1-C_6-2-C_{16}-(ω-COOH)-PC to 1.0 mM for 1-C_8-2-C_{12}-(ω-COOH)-PC. The addition of each two methylenes in the *sn*-2 chain decreased the CMC approximately by a factor of 10, which is consistent with the trend observed for a saturated short-chain diacyl-PC series (Bian & Roberts, 1992; Tausk et al., 1974a,b). CMCs were higher for the 1-acyl-2-acyl-(ω-COOH)-PC compounds than would be expected for a comparable length PC with saturated fatty acyl chains [e.g., 1-C_8-2-C_{12}-(ω-COOH)-PC versus 1-C_8-2-C_{12}-PC]. The terminal carboxylate is hydrophilic and to orient it at the surface, other methylene carbons are likely to be at the surface as well. Additionally, for electrostatic reasons, the terminal carboxylate is not likely to orient itself at the interface near the negatively charged phosphate of the headgroup. A preferred orientation might be for the *sn*-2 chain to be splayed out such that it will be in closer proximity to the positively charged quaternary nitrogen of the headgroup of another 1-acyl-2-acyl-(ω-COOH)-PC molecule. This hypothesis is supported by the higher values that were measured for the surface areas of these species (typically 95–105 Å²) relative to typical diacyl-PCs. These values support the assumption that the carboxylate is likely to reside at the surface of these micelles, with that group spread out, thus occupying a greater surface area than a typical diacyl-PC. The R_H values measured for the 1-acyl-2-acyl-(ω-COOH)-PC compounds ranged from ~400 to 600 Å depending on the exact PC concentration and whether or not samples were buffered. These polydisperse species form much larger micelles than what is typically seen with diacyl-PCs (for diC_7PC, R_H ~75 Å at a similar concentration).

Table 2: ^{13}C NMR Spin–Lattice Relaxation Times for 1-C_8-2,2′-C_{12}-1′-C_8-PC in CD_3OD

carbon atom	T_1 (s)
backbone	
CHO	0.63
CH_2OP	0.40
CH_2O	0.37
headgroup	
CH_2N	0.98
CH_2OP	0.92
$N(CH_3)_3$	0.95
chains[a]	
α (*sn*-2)	1.23
α (*sn*-1)	1.02
β	1.38
$(CH_2)_n$	1.26, 1.32[b]
ω-2 (*sn*-1)	3.19
ω-1 (*sn*-1)	4.12
ω (*sn*-1)	5.72

[a] Chains are numbered α–ω where the α-carbon is next to the ester linkage and the ω-carbon is the terminal methyl carbon. [b] Two closely spaced resonances occur for the $(CH_2)n$; the T_1's are similar but not quite identical.

^{13}C NMR Measurement of Spin–Lattice Relaxation Times. T_1 measurements provide information on the relative mobility or rigidity of a given part of a phospholipid molecule. ^{13}C NMR T_1 values were measured for 1-C_8-2,2′-C_{12}-1′-C_8-PC in CD_3OD (Table 2) and for 1-C_8-2-C_{12}-(ω-COOH)-PC (Table 3) in CD_3OD and D_2O. T_1 measurements were performed in both solvents for 1-C_8-2-C_{12}-(ω-COOH)-PC to compare the differences in relaxation times for each species in micellar aggregates (D_2O) as well as for monomers (CD_3OD). The T_1's for the glycerol backbone and headgroup resonances of 1-C_8-2,2′-C_{12}-1′-C_8-PC in CD_3OD ranged from 0.38 to 0.98 s, consistent with acyl chain T_1's for other short-chain PC species. As expected, the *sn*-2 chain carbons have much more restricted motions, with T_1's ranging from 1.23 to 1.38 s; the *sn*-1 chains possess more mobility with T_1's ranging from 1.02 to 6.04 s, the latter value representing the terminal end of that acyl chain. As shown in Table 3, the T_1's for the backbone and headgroup resonances of 1-C_8-2-C_{12}-(ω-COOH)-PC are short (<1 s) regardless of which solvent the lipid is dissolved in, although the trend is toward longer T_1's, representing more mobility, for the monomeric species in organic solvent. For the chain resonances, the T_1's were longer in CD_3OD than D_2O and increased toward the terminus of each chain for each solvent. T_1 values of the CH_2's adjacent to an ionized terminal carboxylate were relatively short (~0.5 s) while those adjacent to a protonated terminal carboxylate were slightly longer (~1.2–1.4 s). This indicates more mobility for the CH_2's next to a protonated terminal carboxylate. Such behavior is consistent with the hypothesis that the chain with an ionized carboxylate is more likely to have a terminus that is anchored at the interface, an orientation which would restrict motion.

Table 3: ^{13}C NMR Spin–Lattice Relaxation Times for 1-C_8-2-C_{12}-(ω-COOH)-PC

carbon atom	T_1 (s) D_2O	T_1 (s) CD_3OD
backbone		
CHO	0.29	0.67
CH_2OP	0.21	0.41
CH_2O	0.18	0.37
headgroup		
CH_2N	0.60	0.89
CH_2OP	0.58	0.92
$^+N(CH_3)_3$	0.73	1.02
chains[b]		
α (*sn*-2)	0.35	0.83
α (*sn*-1)	0.37	0.99
β	0.46	1.15
$(CH_2)_n$	0.79	2.12
ω-2 (*sn*-1)	0.93	3.36
ω-1 (*sn*-1)	1.29	4.56
ω (*sn*-1)	2.52	6.31
α*-protonated (*sn*-2)[c]	1.44	1.20
α*-ionized (*sn*-2)[c]	0.53	
β*-protonated (*sn*-2)[c]	1.21	1.30
β*-ionized (*sn*-2)[c]	0.59	

[a] Sample 20 mM in D_2O; apparent pH 7.5. [b] Acyl chains are numbered α–ω where the α-carbon is next to the ester linkage and the ω-carbon is the terminal methyl. [c] α*-protonated (*sn*-2) refers to the carbon atom directly next to the *sn*-2 terminal COOH moiety; α*-ionized (*sn*-2) refers to the carbon atom directly next to the *sn*-2 terminal COO^- moiety; β*-ionized (*sn*-2) refers to the carbon atom next to the α*-ionized (*sn*-2) moiety.

pK_a of the Terminal Carboxylate in 1-Acyl-2-acyl-(ω-COOH)-PCs. The pK_a of the terminal carboxylate was determined by ^{13}C NMR spectroscopy. There is slow exchange between the CH_2 resonances adjacent to the protonated (36.35 ppm) and ionized (37.76 ppm) carboxylates. These resonances are also separable from the *sn*-1/*sn*-2 α-CH_2 groups adjacent to the ester linkages (34.00, 34.03 ppm). pH titrations of 1-C_8-2-C_{12}-(COOH)-PC were performed, and the integrated intensities of the protonated and ionized forms were quantified. From the Henderson–Hasselbach equation, the pK_a of the terminal carboxylate of 1-C_8-2-C_{12}-(COOH)-PC was calculated to be 7.3 ± 0.3. With this pK_a value, the exact quantities of protonated or ionized forms of the terminal carboxylate in a given sample of 1-C_8-2-C_{12}-(COOH)-PC could be easily determined.

pH-Induced Shifts in 1-Acyl-2-acyl-(ω-COOH)-PCs Aggregate Structure. A sample (5 mM) of 1-C_8-2-C_{12}-(COOH)-PC exhibited a macroscopically observable change in appearance from optically clear to opaque (reminiscent of small unilamellar vesicles) when the pH was changed from 8.2 to 6.1. This was suggestive of a change in aggregate structure. ^{31}P NMR spectroscopy has previously served as a useful tool for discerning different aggregate structures (Seelig et al., 1987; Cullis & de Kruijff, 1979; Burnell et al., 1974; Browning, 1981). Micelles, bilayers, and hexagonal phases each have characteristic spectral patterns. At pH 8.2, the ^{31}P NMR spectrum of 1-C_8-2-C_{12}-(COOH)-PC showed a single sharp (20 Hz) isotropic line which is consistent with moderately large micellar particles (Figure 2A). When the pH was adjusted to 6.1, the ^{31}P NMR spectrum displayed a 2-kHz broad asymmetric spectral pattern, characteristic of a bilayer powder pattern, superimposed on a sharp isotropic line. This indicated that some micelles coexisted with a bilayer aggregate at this pH (Figure 2B). At pH ~6 the carboxylate is primarily protonated (94%) and could possibly be buried in the hydrophobic interior of the aggregate than at the surface. With the long *sn*-2 chain, such a PC would be expected to pack better in bilayer vesicles than in micelles.

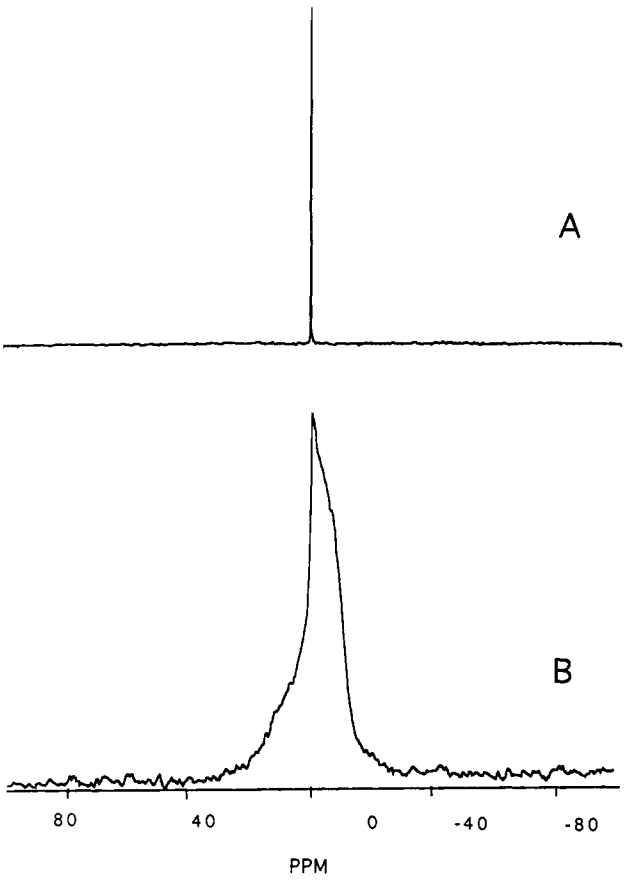

FIGURE 2: ^{31}P NMR (202.3 MHz) spectra of 5 mM 1-C_8-2-C_{12}-(ω-COOH)-PC at (A) pH 8.2 and (B) pH 6.1.

Interactions of 1-C_8-2-C_{12}-(ω-COOH)-PC Micelles with Lanthanide Shift Reagents. Lanthanide shift reagents have been useful in examining different phospholipid aggregates [including short-chain PCs (Gabriel, 1986)] in order to discern the surface accessibility of a given nucleus. Only surface-accessible nuclei will be affected by this water-soluble shift reagent. The addition of a paramagnetic probe to the micellar samples at pH 8 was used to confirm the presence of the *sn*-2 chain terminal carboxylate at the interface of the micelle (Figure 3). This experiment was restricted to samples at pHs above 7.5 (so that most of the terminal carboxylate was ionized) for two reasons: (i) the CH_2 resonances adjacent to protonated ω-carboxylates have ^1H NMR chemical shifts which at neutral or acidic pH values overlap *sn*-1/*sn*-2 α-CH_2 resonances, thus any interactions with the carboxylate could not be discerned from interactions with *sn*-1/*sn*-2 α-CH_2 resonances, and (ii) the ω-1 CH_2 adjacent to the ionized carboxylate has a ^1H NMR shift ~0.25 ppm upfield from the same group in the protonated carboxylate PC, thus specific interactions of Pr^{3+} with the ionized carboxylate can be observed. Pr^{3+} (0.1–1 mM) was titrated into a 5 mM sample of 1-C_8-2-C_{12}-(ω-COOH)-PC at pH 7.67 (Figure 3). Line widths broadened for all resonances. Chemical shift changes, which are characteristic of H_2O-accessible nuclei in PC micelle or small vesicle/Pr^{3+} titrations, were not observed for any resonances. Rather, upon addition of increasing amounts of Pr^{3+}, there was a preferential loss of integrated intensity for the CH_2 groups next to the terminal carboxylate (indicated by the arrows in Figure 3). Those resonances lost significantly more intensity than the α-CH_2 *sn*-2 resonance, which is in the interfacial region. As a control, the same Pr^{3+} titration was performed with diC_7PC micelles (data not shown). For diC_7-

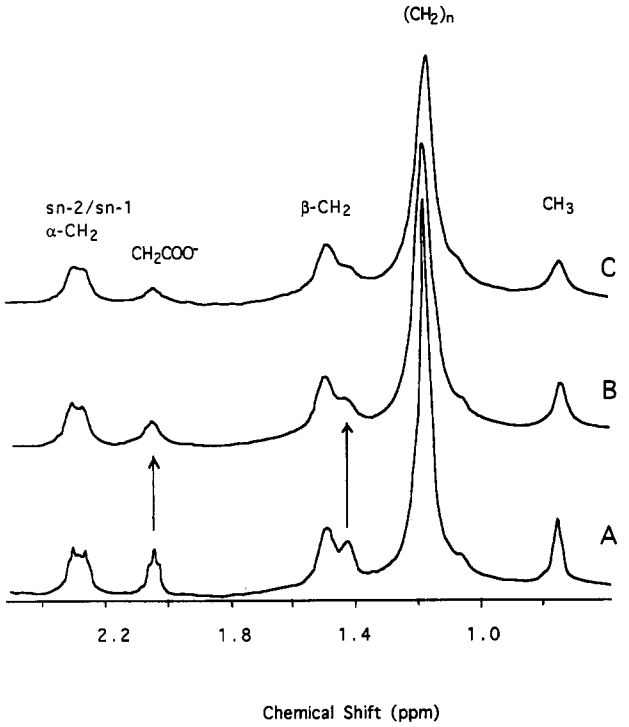

FIGURE 3: ^{1}H NMR (500 MHz) spectra of 5 mM 1-C_8-2-C_{12}-(ω-COOH)-PC (pH 8) in the presence of (A) 0, (B) 0.1, and (C) 0.2 mM Pr^{3+}.

PC, the $N(CH_3)_3$ resonance shifted 0.02 ppm downfield and broadened by 17 Hz, while α and β chain resonances also shifted 0.01–0.04 ppm and also broadened by 16–20 Hz with increasing amounts of Pr^{3+} (0.1–1 mM). In the case of di-C_7PC, the α-CH_2's did not lose intensity as those near the free carboxylate in 1-C_8-2-C_{12}-(ω-COOH)-PC. The Pr^{3+} titrations were repeated but followed by ^{31}P NMR spectroscopy. Addition of 0.5 mM Pr^{3+} to di-C_7PC resulted in a 28-Hz broadening of the ^{31}P resonance as well as a 2.14 ppm upfield change in chemical shift, indicative of a strong interaction of Pr^{3+} with the phosphate of the headgroup. The same concentration of Pr^{3+} added to 1-C_8-2-C_{12}-(ω-COOH)-PC micelles resulted in a 0.05 ppm upfield chemical shift and a 10-Hz broadening of the phosphorus group. These results indicate that the terminal carboxylate is at the interface and interacts preferentially with the Pr^{3+} ions. Phospholipase A_2 requires Ca^{2+} for activity; hence the affinity of the terminal carboxylate of 1-C_8-2-C_{12}, (ω-COOH)-PC for ions may be critical for interpreting the enzyme kinetics.

Hydrolysis of Bolaform and 1-Acyl-2-acyl-(ω-COOH)-PCs by Phospholipase A_2 (Naja naja naja). The bolaform or covalent dimer PCs were initally examined as substrates for phospholipase A_2 in the presence of 5 mM Ca^{2+}, a typical concentration used in pH-stat assays of this enzyme. This amount of Ca^{2+} is in considerable excess over what is needed to saturate the enzyme. As shown in Figure 4, when 0.64 μg of phospholipase A_2 was added to a 5 mM sample of 1-C_8-2,2′-C_{12}-1′-C_8-PC, hydrolysis proceeded with an initial burst phase (typically ~500 μmol min^{-1} mg^{-1}), followed by a lower rate (typically ~100 μmol min^{-1} mg^{-1}). When more phospholipase A_2 (0.65 μg at t = 10, and 2 μg at t = 25 min) was added to the same sample, the same biphasic response was again observed. [If enzyme was added to the bolaform solution in the presence of EDTA or to an aqueous solution of pH 8.0, there was no change in pH (e.g., no addition of NaOH), indicating that the burst phase was due to enzymatic hydrolysis of lipid.] This behavior is consistent with phospholipase A_2

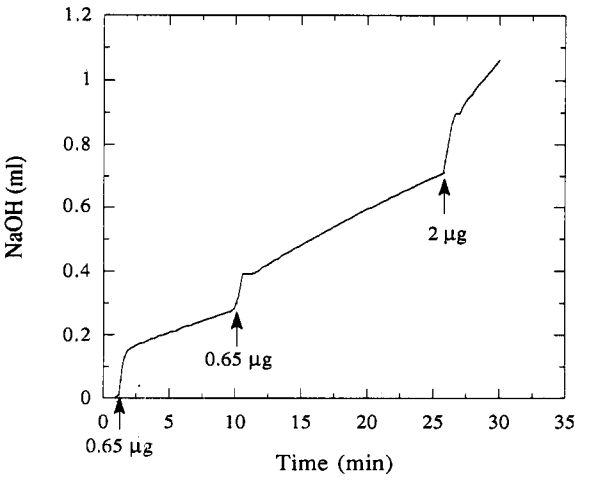

FIGURE 4: pH-stat titration profile of phospholipase A_2 hydrolysis of 5 mM 1-C_8-2,2′-C_{12}-1′-C_8-PC, in the presence of 5 mM Ca^{2+}. The arrows indicate the addition of phospholipase A_2 (*Naja naja naja*) in the amounts indicated.

either (i) adsorbed to a specific micelle and only slowly diffusing to another substrate pool or (ii) inhibited by product 1-C_8-2-C_{12}-(ω-COOH)-PC. For this sample, 35.9% of the total available PC was hydrolyzed over a 30-min incubation period at rates which strongly depended on how much phospholipase A_2 was added. Since <50% of the available *sn*-2 acyl linkages available were cleaved over a reasonable period of time, it was suspected that phospholipase A_2 hydrolysis of the bolaform PCs under these particular experimental conditions yielded water-soluble lyso-PC and a new PC substrate with a carboxylic acid in the terminus of the *sn*-2 chain as products rather than lyso-PC and a dicarboxylic acid. These initial results suggested that the 1-acyl-2-acyl-(ω-COOH)-PC generated *in situ* by phospholipase A_2 hydrolysis of the bolaform PCs was not a good substrate for phospholipase A_2, at least not under the conditions of this assay.

pH-stat studies of phospholipase A_2 activity toward the bolaform PC were performed at both lower and higher levels of Ca^{2+} to investigate the possibility that Ca^{2+} levels might affect hydrolysis rates. This was particularly relevant since the 1-acyl-2-acyl-(ω-COOH)-PC product, predominantly negatively charged at pH 8.0, has the potential for strong chelation of Ca^{2+}. Figure 5A shows pH-stat titration profiles of phospholipase A_2 toward 5 mM 1-C_8-2,2′-C_{12}-1′-C_8-PC samples with 0.1 and 10 mM Ca^{2+} present. With low Ca^{2+} in the assay mix, 93% of the substrate was hydrolyzed, with an initial rate of 570 μmol min^{-1} mg^{-1}. At 0.1 mM Ca^{2+}, both halves of the dimer were hydrolyzed. In the presence of 10 mM Ca^{2+}, only 43% of the *sn*-2 linkages were hydrolyzed at a rate of 174 μmol min^{-1} mg^{-1} (after the initial burst phase). This titration profile shows the same biphasic behavior previously described for 1-C_8-2,2′-C_{12}-1′-C_8-PC samples with 5 mM Ca^{2+} present.

Chemically synthesized 1-acyl-2-acyl-(ω-COOH)-PC micelles were examined independently as substrates for phospholipase A_2. The region from 0 to 6 min in Figure 6 shows the result of the addition of 2 μg of phospholipase A_2 to a 5 mM sample of 1-C_8-2-C_{12}-(ω-COOH)-PC in the presence of 5 mM Ca^{2+}. No significant hydrolysis of this substrate occurred under these conditions (specific activity <5 μmol min^{-1} mg^{-1}), with less Ca^{2+}, more Ca^{2+}, or prolonged incubation times (>30 min). To determine whether or not these species were binding to the active site, the activity of phospholipase A_2 was measured toward mixed micelles of

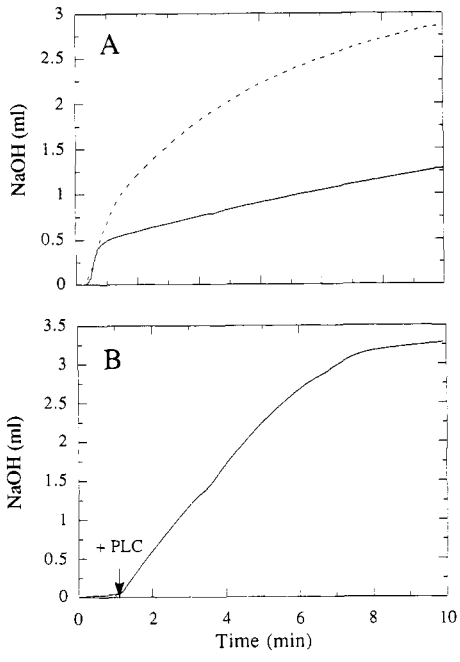

FIGURE 5: pH-stat titration profile of 5 mM 1-C_8-2,2′-C_{12}-1′-C_8-PC after the addition of (A) 2 μg of phospholipase A_2 (*Naja naja naja*) and 0.1 mM Ca^{2+} (- - -) or 10 mM Ca^{2+} (—), or (B) 1.2 μg of phospholipase C (*B. cereus*).

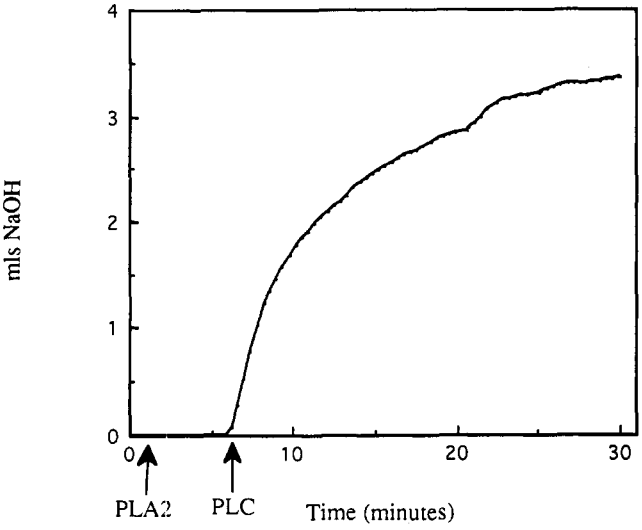

FIGURE 6: pH-stat titration profile of 5 mM 1-C_8-2-C_{12}-(ω-COOH)-PC upon the addition of 2 μg of phospholipase A_2 (*Naja naja naja*) and 1.2 μg of phospholipase C (*B. cereus*).

diheptanoyl-PC micelles and the 1-acyl-2-acyl-(ω-COOH)-PCs (Table 4). Each 1-acyl-2-acyl-(ω-COOH)-PC in the series was a potent inhibitor of phospholipase A_2 hydrolysis of diheptanoyl-PC micelles, but only when the carboxylate species was near or above its CMC. For example, inhibition of diheptanoyl-PC hydrolysis by greater than 90% occurred at ~1 mM 1-C_8-2-C_{12}-(ω-COOH)-PC (CMC_{H_2O} = 1.01 mM in water), ~100 μM 1-C_8-2-C_{14}-(ω-COOH)-PC (CMC_{H_2O} = 90 μM in water), and ~50 μM 1-C_6-2-C_{16}-(ω-COOH)-PC (CMC_{H_2O} = 22 μM in water). At the pH of the assays, the 1-acyl-2-acyl-(ω-COOH)-PC species would have higher CMC values than in water (see Table 1), but the presence of the micellar di-C_7PC substrate should lower these values. It should be noted that this inhibition occurs irrespective of the level of Ca^{2+} present, since similar results were generated at 0.1, 10, and 100 mM Ca^{2+} (data not shown). Collectively, these data suggested that the 1-acyl-2-acyl-(ω-COOH)-PC series form

Table 4: Inhibition of Phospholipase A_2 (*Naja naja naja*) Catalyzed Hydrolysis of 5 mM Diheptanoyl-PC Micelles by 1-Acyl-2-acyl-(ω-COOH)-PC Species[a]

inhibitor (mM)	specific activity (μmol min^{-1} mg^{-1}) 1-C_8-2-C_{12}-(ω-COOH)-PC	1-C_8-2-C_{14}-(ω-COOH)-PC	1-C_6-2-C_{16}-(ω-COOH)-PC
0	1625 (178)[b]	2170 (117)	2170 (117)
0.01	1765 (112)	1790 (57)	306 (21)
0.05	2130 (200)	1244 (359)	89 (4)
0.10	2114 (184)	152 (38)	2.3 (2.3)
1.00	3.5 (3.5)	0 (0)	6.4 (6.4)

[a] All assays contain 0.1 mM Ca^{2+}; 0.65 μg of phospholipase A_2 was added to initiate hydrolysis. Note that inhibition only occurs near the CMC of the 1-C_x-2-C_y-(ω-COOH)-PC species added. [b] Values in parentheses reflect the error range from assays performed in triplicate or duplicate.

negatively charged mixed micelles that bind phospholipase A_2 tightly, with the 1-acyl-2-acyl-(ω-COOH)-PC binding to the enzyme in such a way as to render it nearly inactive.

Long-chain bolaform PCs have been synthesized as probes of the importance of lipid extraction in enzyme kinetics. These species when present in vesicles or in detergent mixed micelles were found to be extremely poor substrates for phospholipase A_2 (L. Cuccia, N. Hebert, A. Beck, G. Just, and R. B. Lennox, unpublished results]. Part of this may be due to orientational aspects of the long-chain bolaform lipid which in vesicles can either span the bilayer or adopt a U-shaped conformation. In view of the extreme potency observed for 1-acyl-2-acyl-(ω-COOH)-PC inhibition of the enzyme, an alternative interpretation is possible. The product 1-acyl-2-acyl-(ω-COOH)-PC from such a bolaform will have a very low CMC. If it has comparable inhibition potency to the shorter chain analog, one would not observe much phospholipase A_2 activity, either under high or low Ca^{2+} conditions.

Hydrolysis of Bolaform and 1-Acyl-2-acyl-(ω-COOH)-PCs by Phospholipase C (B. cereus). There are two potential phospholipase C cleavage sites in the bolaform PC. Both glycerophosphate headgroups were efficiently and completely cleaved upon the addition of phospholipase C (Figure 5B). The initial rate of ~1600 μmol min^{-1} mg^{-1} was comparable to that of the enzyme toward di-C_7PC (a reference compound with no tethered chains). The bolaform PC has structural properties consistent with previously determined requirements for rapid phospholipase C hydrolysis, namely, a certain degree of hydrophobicity in the acyl chain region which is nonspecific to chain length and an *sn*-2 carboxylic ester group (Lewis et al., 1990; Burns et al., 1981).

The ω-carboxylate PC was also an excellent substrate for phospholipase C (Figure 6). 100% of the substrate was rapidly hydrolyzed at an initial rate of comparable to that of the enzyme toward the bolaform or di-C_7PC. The sample had 5 mM Ca^{2+} present as a requisite for phospholipase A_2 hydrolysis, but this cation is unnecessary for phospholipase C hydrolysis. The presence of the Ca^{2+} neither adversely affected nor enhanced phospholipase C hydrolysis when compared to samples run without Ca^{2+} (data not shown). This is further evidence that Ca^{2+} does not dramatically alter the phase of this PC.

Lipid Mixing of Bolaform and 1-C_8-2-C_{12}-(ω-COOH)-PC. The peculiar inhibitory behavior of the ω-carboxylate PCs could reflect strange mixing behavior of this anionic lipid with PC substrate molecules for the enzyme. To address this, we have examined the extent and rapidity of lipid mixing in these short-chain PC micelles. The probe molecule used for these experiments was 1-C_8-2-C_4pyr-PC. The CMC of this

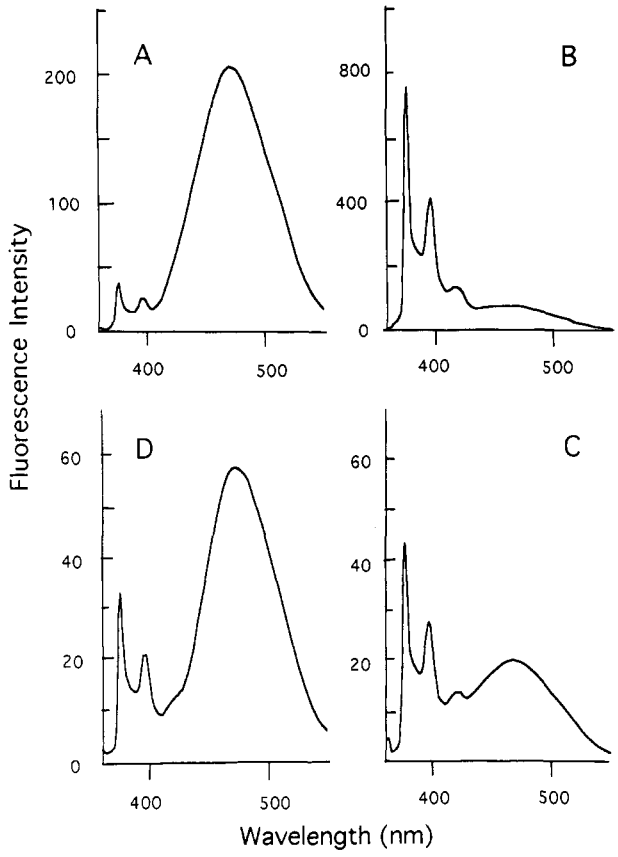

FIGURE 7: Fluorescence spectra of 1-C_8-2-C_4pyr-PC (0.08 mM) (A) alone, and mixed with (B) 0.5 mM 1-C_8-2,2′-C_{12}-1′-C_8-PC, (C) 2.5 mM 1-C_8-2-C_{12}-(ω-COOH)-PC, or (D) 0.5 mM 1-C_8-2,2′-C_{12}-1′-C_8-PC and 0.5 mM 1-C_8-2-C_{12}-(ω-COOH)-PC.

compound was less than 0.001 mM, and at concentrations above this (0.1–0.3 mM solutions were used in the experiments) the fluorophore packed in micelles gave rise to a large excimer band (470 nm) with only a small monomer band at 380 nm (Figure 7A). This fluorescent phospholipid (0.08 mM) mixed well with bolaform 1-C_8-2,2′-C_{12}-1′-C_8-PC (0.5 mM) as monitored by the disappearance of the excimer band and the increase in monomer bands (Figure 7B). Mixing of the pyrene probe micelles with 2.5 mM 1-C_8-2-C_{12}-(ω-COOH)-PC also occurred (Figure 7C), but to a smaller extent, since more excimer fluorescence was observed. At pH 8, pure 1-C_8-2-C_{12}-(ω-COOH)-PC has a CMC of ~4 mM. Since there was a significant decrease in the pyrene excimer band (i.e., compared Figure 7 A with panel C), the CMC of the ω-COOH-PC must have been depressed by the pyrene-PC. The addition of 0.1 mM Ca^{2+} had no significant effect on the spectrum of the pyrene-PC diluted with 1-C_8-2-C_{12}-(ω-COOH)-PC at pH 8. Higher concentrations (e.g., 2–5 mM) of Ca^{2+} added to (ω-COOH)-PC micelles led to precipitation in the sample. A quite different situation occurred when the fluorophore was initially mixed with the bolaform PC or diheptanoyl-PC and that mixed micelle system was subsequently diluted with 1-C_8-2-C_{12}-(ω-COOH)-PC micelles. When the bolaform/1-C_8-2-C_4pyr-PC mixed micelle was mixed with 1-C_8-2-C_{12}(ω-COOH)-PC [final concentrations were 0.5 mM 1-C_8-2,2′-C_{12}-1′-C_8-PC, 0.08 mM 1-C_8-2-C_4pyr-PC, and 0.5 mM 1-C_8-2-C_{12}-(ω-COOH)-PC], the fluorophore excimer band, rather than decreasing further (as would be expected if all the components mixed randomly—the ratio of the monomer to excimer band should have increased from the value exhibited by Figure 7B), actually increased and concurrently the monomer also decreased (Figure 7D). A quantitative comparison of the I_{380}/I_{470} values, which measures the extent of mixing in these steady-state fluorescence experiments, is shown in Table 5. To see if this was a more general phenomenon with other short-chain PCs as well as the bolaform, we examined the steady-state mixing of the 1-C_8-2-C_4pyr-PC/di-C_7PC micelles [which exhibit a large monomer band initially (Figure 8A)] with 1-C_8-2-C_{12}-(ω-COOH)-PC. The final concentrations in the mixture were 2.5 mM di-C_7PC and 0.08 mM 1-C_8-2-C_4pyr-PC without (Figure 8A) and with (Figure 8B) 0.5 mM 1-C_8-2-C_{12}-(ω-COOH)-PC. In this system as well, the excimer band also increased relative to the monomer band upon the addition of the ω-COOH-PC. Such behavior is indicative of a discrete interaction between the bolaform (or di-C_7PC) and 1-C_8-2-C_{12}-(ω-COOH)-PC, which excludes the pyrene-labeled PC probe. Substitution of a fatty acid (e.g., heptanoate) or longer chain lyso-PC which would also partition in the micelles did not cause a segregation of the fluorescent 1-C_8-2-C_4pyr-PC probe from the other components.

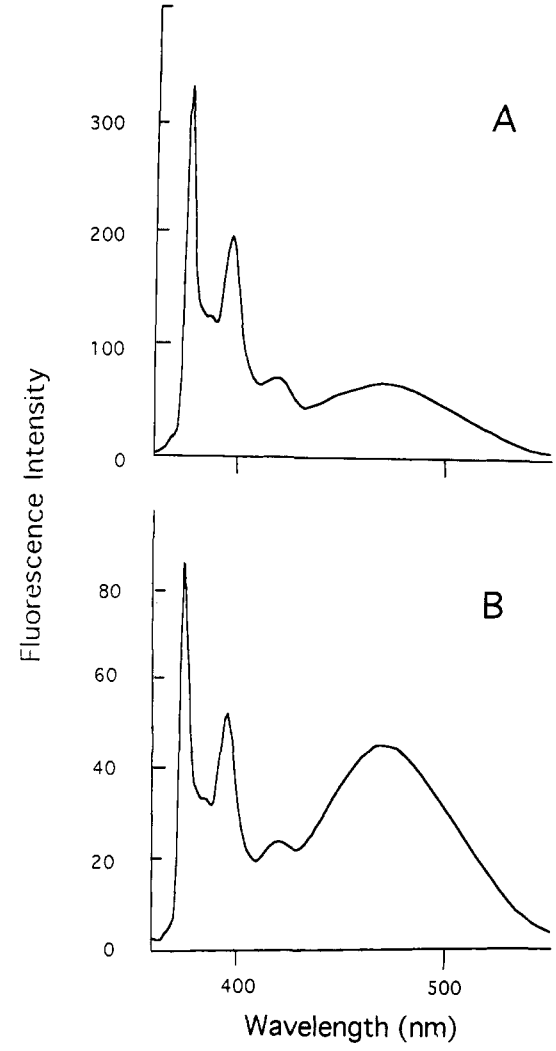

FIGURE 8: Fluorescence spectra of 1-C_8-2-C_4pyr-PC (0.08 mM) (A) in mixed micelles with 2.5 mM di-C_7PC, and (B) mixed with 2.5 mM di-C_7PC and 0.5 mM 1-C_8-2-C_{12}-(ω-COOH)-PC.

The time scale of mixing of micellar components was monitored by stopped-flow fluorescence spectroscopy and examining the change in intensity of the 1-C_8-2-C_4pyr-PC monomer band as a function of time after rapid mixing. When the pyrene PC probe was mixed with di-C_7PC (final lipid concentrations of 0.08 and 2.5 mM, respectively), the increase in the monomer band (Figure 9A) was well fit by the equation

Table 5: Fluorescence Intensity Ratio of 1-C_8-2-C_4pyr-PC (0.08 mM) Monomer to Excimer Band as a Function of Micelle Diluent

diluent PC	I_{380}/I_{470}	k (s^{-1})[a]	[micellar diluent]/[pyr-PC][b]
–	0.17	–	0
di-C_7PC (2.5 mM)	4.63	23	1.0/0.04
$C_8C_{12}C_8$-PC (0.5 mM)	5.95	0.76 ± 0.14	0.46/0.04
C_8C_{12}-(ω-COOH)-PC (2.5 mM)	2.05	1.82 ± 0.14	–[c]
C_8C_{12}-(ω-COOH)-PC + 0.1 mM Ca^{2+}	2.62	–	–[c]
$C_8C_{12}C_8$-PC (0.5 mM)/C_8C_{12}-(ω-COOH)-PC (0.5 mM)	0.57	0.23 ± 0.10[d]	
$C_8C_{12}C_8$-PC (0.5 mM)/ C_8C_{12}-(ω-COOH)-PC (0.5 mM) + 0.1 mM Ca^{2+}	0.65	0.11[d]	
$C_8C_{12}C_8$-PC (0.5 mM)/ C_8C_{12}-(ω-COOH)-PC (0.5 mM) + 5 mM Ca^{2+}	1.17	–	

[a] The exponential rate constant for mixing of pyrene-PC with diluent is calculated from stopped-flow experiments with the ratio of micellar diluent to pyrene-PC shown in the adjacent column. Errors shown are from averages of multiple stopped-flow runs. The actual exponential fits for each curve were considerably better (typically under 10% or less). [b] Micellar diluent is calculated by substracting the CMC from the total concentration of PC. [c] The CMC value is 4.4 mM in Tris, pH 8.0 and 1.0 in water (see Table 1); however, the presence of other lipids lowers the CMC of this compound. Since we cannot determine the effective monomer concentration in these mixtures, the ratio of micellar diluent to the pyrene-PC cannot be calculated. [d] The bolaform and ω-COOH-PC were cosolubilized in one syringe and mixed with the pyrene-PC (in a separate syringe).

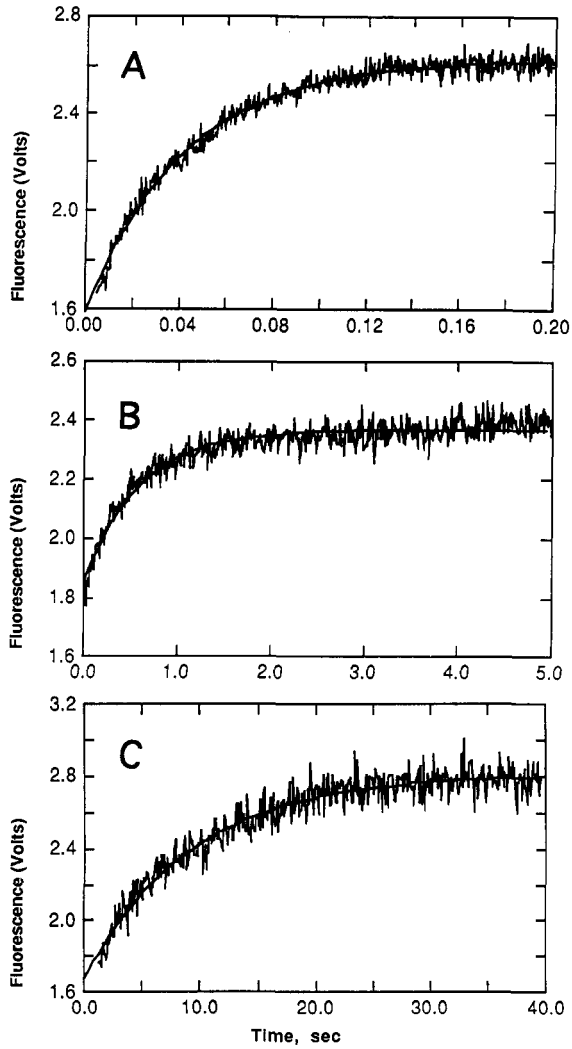

FIGURE 9: Stopped-flow time course for production of monomer band (380 nm) from dilution of 0.16 mM 1-C_8-2-C_4pyr-PC with an equal volume of (A) 5 mM di-C_7PC, (B) 5 mM 1-C_8-2-C_{12}-(ω-COOH)-PC, and (C) 1 mM 1-C_8-2,2′-C_{12}-1′-C_8-PC/1 mM 1-C_8-2-C_{12}-(ω-COOH)-PC mixed micelles. Curves drawn through the data are from a fit with the equation (fluorescence = $A - Be^{-kt}$). Note the three different time scales for mixing of the three samples.

F (fluorescence) = $A - Be^{-kt}$, i.e., a single-exponential rate constant of 23 s^{-1} characterized the mixing of the pyrene-PC with that short-chain PC. Mixing of the fluorophore with either 1 mM of the pure bolaform or 5 mM of the ω-COOH species (Figure 9B) occurred at significantly slower rates (k = 0.76 ± 0.14 s^{-1} and 1.81 ± 0.14 s^{-1} for the bolaform and ω-COOH PC, respectively). The time scale for micellar PC mixing should be compared with the turnover number of the enzyme (~450 s^{-1} for di-C_7PC). Thus, to the extent that the 1-C_8-2-C_4pyr-PC mimics the other short-chain PC species, the enzyme can hydrolyze ~20 substrate molecules before mixing occurs, but given the moderate size of a di-C_7PC micelle (~100–200 molecules/micelle (Lin et al., 1987), there should be a large number of other PC substrate molecules available for the enzyme. Substrate depletion in this PC micelle should not be a problem initially. For both bolaform and ω-COOH phospholipids, the slower mixing times suggest that considerable hydrolysis can occur before lipids are exchanged between different micelles. If enzyme dissociation from these micelles does not occur readily, the phospholipase hydrolysis rates would be expected to decrease as substrate depletion becomes a significant factor.

While mixing of pyrene-PC micelles with pure bolaform or 1-C_8-2-C_{12}-(ω-COOH)-PC was slow, when the two components were cosolubilized in mixed micelles [e.g., adding the pyrene-labeled probe to bolaform/1-C_8-2-C_{12}-(ω-COOH)-PC mixed micelles], there was more than an order of magnitude further decrease in the rate constant for lipid mixing (Figure 9C and Table 5). Under these conditions there was a small decrease in the excimer band and increase in the monomer band when the pyrene probe was added to the bolaform/1-C_8-2-C_{12}-(ω-COOH)-PC mixed micelles, indicating some mixing of lipid components, but the rate constant describing that interaction was ~0.2 s^{-1}. In other words, the bolaform/1-C_8-2-C_{12}-(ω-COOH)-PC mixed micelle did not have the characteristics of either pure component. This behavior was only observed when the ω-COOH-PC was above its CMC. Monomeric ω-COOH-PC had no effect on the bolaform (or di-C_7PC)/pyrene-PC mixing rate (data not shown). Ca^{2+} added to the system decreased the mixing rate to 0.1 s^{-1} (Table 5).

DISCUSSION

Micelle-forming phospholipids have been extremely useful in probing phospholipase interactions. Short-chain PC micelle fusion and monomer–micelle exchange occur relatively rapidly. For PC species with ≤8 carbons in each fatty acyl chain, the products of phospholipase A_2 hydrolysis are water-soluble. Since they do not build up in the micelle, they cannot be interfacial inhibitors of the enzyme. Any inhibition observed must be due to a direct enzyme–product interaction. This is not the case with long-chain lipids, where both the lysophospholipid and the long-chain fatty acid remain partitioned on the vesicle or in the detergent mixed micelle. Short-chain

bolaform and 1-acyl-2-acyl-(ω-COOH)-PC species are novel lipid structures whose micellar nature can be used to address several important questions concerning the interfacial action of phospholipase A_2. (i) 1-Acyl-2-acyl-(ω-COOH)-PC, the product of the bolaform cleavage, has a fatty acid moiety which is intimately linked with another substrate. In a wide variety of other assay systems, it has been observed that fatty acids (particularly unsaturated ones) are inhibitory, although the exact mechanism of this is still a controversy. With symmetric short-chain PCs the product fatty acid is monomeric and partitions into the bulk solution under initial rate assay conditions. Are there conditions where a fatty acid product remains associated with the micelle and is observed to be inhibitory? If so, is it more or less inhibitory than long-chain fatty acids added to the assay mix? (ii) Does phospholipase A_2 hydrolyze substrate PC in micelles in a processive, a dissociative mode, or both? (iii) The phospholipase A_2 transition state analog crystal structure showed a hydrophobic binding pocket for ~8 carbons. This was used to suggest that lipid extraction from the micelle into this pocket would be a critical part of the enzyme's action. If the *sn*-2 chains of two molecules are tethered, what is the effect on the observed enzymatic hydrolysis rate?

The bolaform PC has two cleavage sites—hydrolysis of the first ester bond produces a water-soluble lyso-PC (which should readily dissociate from the micelle) and 1-acyl-2-acyl-(ω-COOH)-PC which may also be hydrolyzed by the enzyme (producing the same water-soluble lyso-PC and a water-soluble dicarboxylic acid). Under low Ca^{2+} where the secondary substrate is monomeric, the bolaform PC can be completely hydrolyzed by the enzyme. The rate is certainly not constant (rate profiles are markedly curved), but all available fatty acyl linkages are hydrolyzed. As the Ca^{2+} is increased, the 1-acyl-2-acyl-(ω-COOH)-PC remains associated with the micelle after it is generated enzymatically and is inhibitory to phospholipase A_2, producing biphasic reaction kinetics. NMR experiments clearly show the surface accessibility of the ω-carboxylate group when packed in micelles. However the ω-COOH-PC is arranged in the micelle, it is no longer a good substrate for phospholipase A_2. Furthermore, ω-COOH-PC interacts strongly with the bolaform (as well as di-C_7PC) as shown by the fluorescence steady-state and stopped-flow experiments. These observations must be important, since only the micellar product of bolaform hydrolysis is a potent inhibitor of phospholipase A_2 activity. Micellar 1-C_8-2-C_{12}-(ω-COOH)-PC traps the enzyme and prevents it from interacting with added micellar PC. This type of kinetic trapping of phospholipase A_2 has been seen in anionic vesicle systems, and this is a clear example of such kinetic behavior in a PC micelle.

Under high Ca^{2+} conditions, about 5% of the total bolaform ester bonds are rapidly hydrolyzed before the rate slows dramatically. Furthermore, with each microgram quantity of enzyme added to millimolar substrate, another 5% of the bolaform substrate is hydrolyzed before the abrupt slowing of the observed rate. Whether the slow rate phase represents enzyme desorption or 1-acyl-2-acyl-(ω-COOH)-PC exchange is not clear at this time. If the same proportion of bolaform and 1-C_8-2-C_{12}-(ω-COOH)-PC were cosolubilized, no initial "burst" phase was observed. These observations are consistent with (i) a nonrandom distribution of the 1-C_8-2-C_{12}-(ω-COOH)-PC when generated *in situ* and with (ii) bolaform/1-C_8-2-C_{12}-(ω-COOH)-PC/Ca^{2+} complexes binding to the enzyme in such a way as to inhibit the enzyme and prevent it from desorbing and interacting with other PC substrate molecules. The fluorescence experiments are also consistent with a nonrandom distribution of lipids. A bolaform (or diheptanoyl-PC)/1-C_8-2-C_{12}-(ω-COOH)-PC complex once formed (with or without Ca^{2+}) does not reorganize rapidly with added pyrene-labeled PC. If comparable amounts of 1-acyl-2-acyl-(ω-COOH)-PC and a good PC substrate (e.g., di-C_7PC) are comixed, enzyme activity is inhibited and, under these conditions, the kinetics are no longer biphasic.

The inhibition potency of the micellar 1-acyl-2-acyl-(ω-COOH)-PC suggests a very specific arrangement of this molecule bound to the enzyme. Perhaps the free carboxylate of 1-acyl-2-acyl-(ω-COOH)-PC binds to the enzyme in such a way as to misalign the *sn*-2 ester bond in the active site so that it is no longer a substrate. The mole fraction micellar 1-acyl-2-acyl-(ω-COOH)-PC necessary for 50% inhibition of phospholipase A_2 hydrolysis of di-C_7PC is <0.02. In fact, for the 1-C_6-2-C_{16}-(ω-COOH)-PC species it is well under 0.002. As either the *sn*-1 or the *sn*-2 chain is lengthened, one would expect an even more potent inhibitor. A short-chain PC such as the bolaform PC can be introduced into membranes if added mixed with gel-state long-chain PCs (Gabriel, 1986). Hydrolysis of such an exogenous bolaform would generate a product which should inhibit phospholipase A_2 *in situ*.

The initial hydrolysis rate toward the bolaform PC allows us to assess the importance of impaired lipid extraction for phospholipase A_2 action. If phospholipase A_2 activity toward 1-C_8-2,2′-C_{12}-1′-C_8-PC (under low Ca^{2+} conditions) is compared to di-C_7PC, one sees a 4-fold decrease in specific activity. The surface that the enzyme sees has the same phosphocholine headgroups whether one is comparing the bolaform or the di-C_7PC. A major difference in the two micelles is a damping of *sn*-2 chain segmental motions in the bolaform molecules. The creation of a PC dimer will also affect both the lateral and vertical diffusion of the molecule. Tethering the molecule should make it more difficult for the enzyme to extract a substrate from the micelle surface. The contribution this has to the observed rate is hard to assess, but the 4-fold decrease is consistent with the enzyme having to extract part of a larger molecule as it tries to align a headgroup and the *sn*-2 acyl chain into the active site. Similar dimeric PCs have been constructed with either *sn*-1 or *sn*-2 thiols at the chain terminus for disulfide cross-linking (Soltys et al., 1993). Phospholipase A_2 rates toward those disulfide dimers are 1–7% of the rate of the enzyme toward the reduced species. The addition of a rigid disulfide link at the chain terminus should further decrease the ease of extraction of a PC, compared to the bolaform examined in this work.

ACKNOWLEDGMENT

We thank Prof. Sow-Hsin Chen and Mr. Bruce Carvalho of the Department of Nuclear Engineering, MIT, for the use of their QLS spectrometer. We also thank Dr. R. Bruce Lennox, McGill University, for discussions of his work on long-chain bolaform PCs.

REFERENCES

Adamich, M., Roberts, M. F., & Dennis, E. A. (1979) *Biochemistry 18*, 3308–3314.

Berchtold, R. (1981) *Chem. Phys. Lipids 18*, 55–60.

Berg, O. G., Yu, B.-Z., Rogers, J., & Jain, M. K. (1991) *Biochemistry 30*, 7283–7297.

Bian, J., & Roberts, M. F. (1991) *J. Phys. Chem. 95*, 2572–2577.

Bian, J., & Roberts, M. F. (1992) *J. Colloid Interface Sci. 153*, 420–428.

Bradford, M. M. (1976) *Anal. Biochem. 72*, 248–254.
Browning, J. L. (1981) in *Liposomes: From Physical Structure to Therapeutic Applications* (Knight, C. G., Ed.) pp 177–218, Academic Press, New York.
Burack, W. R., Yuan, Q., & Biltonen (1993) *Biochemistry 32*, 583–589.
Burnell, E. E., Cullis, P. R., & de Kruijff, B. (1974) *Biochim. Biophys. Acta 603*, 63–69.
Burns, R. A., Jr., & Roberts, M. F. (1980) *Biochemistry 19*, 3100–3106.
Burns, R. A., Jr., Friedman, J. M., & Roberts, M. F. (1981) *Biochemistry 20*, 5945–5950.
Burns, R. A., Donovan, J. M., & Roberts, M. F. (1983) *Biochemistry 22*, 964–973.
Chen, P. S., Toribara, T. Y., & Warner, H. (1956) *Anal. Chem. 28*, 1756–1758.
Cullis, P. R., & de Kruijff, B. (1979) *Biochim. Biophys. Acta 559*, 399–420.
Dennis, E. A. (1973) *J. Lipid Res. 14*, 152–159.
Dennis, E. A., & Pluckthun, A. (1986) in *Enzymes of Lipid Metabolism* (Freysz, L., & Gatt, S., Eds.) pp 121–132, Plenum Press, New York.
Findlay, A. (1972) *Findlay's Practical Physical Chemistry*, 9th ed., John Wiley & Sons, New York.
Gabriel, N. E. (1986) Ph.D. Dissertation, Massachusetts Institute of Technology, Cambridge, MA.
Ghomashchi, F., O'Hare, T., Clary, D., & Gelb, M. H. (1991a) *Biochemistry 30*, 7298–7305.
Ghomashchi, F., Yu., B.-Z., Berg, O. G., Jain, M. K., & Gelb, M. H. (1991) *Biochemistry 30*, 7318–7329.
Hebert, N., Beck, A., Lennox, R. B., & Just, G. (1992) *J. Org. Chem. 57*, 1777–1793.
Jain, M. K., Yuan, W., & Gelb, M. (1989) *Biochemistry 28*, 4135–439.
Jain, M. K., Ranadive, G. N., Yu., B.-Z., & Verheij, H. M. (1991a) *Biochemistry 30*, 7330–7340.
Jain, M. K., Rogers, J., Berg, O. G., & Gelb, M. H. (1991b) *Biochemistry 30*, 7340–7348.
Jain, M. K., Yu, B.-Z., Rogers, J., Ranadive, G. N., & Berg, O. G. (1991c) *Biochemistry 30*, 7306–7317.
Jain et al. (1992) *Biochemistry 31*, 7841–7847.
Lewis, K. A., Bian, J., Sweeney, A., & Roberts, M. F. (1900) *Biochemistry 29*, 9962–9970.
Lin, T.-L., Chen, S.-H., & Roberts, M. F. (1987) *J. Am. Chem. Soc. 109*, 2321–2328.
Roberts, M. F., Adamich, M., Robson, R. J., & Dennis, E. A. (1979) *Biochemistry 18*, 3301–3307.
Scott, D. L., White, S. P., Otwinoski, Z., Yuan, W., Gelb, M. H., & Sigler, P. B. (1990) *Science 250*, 1541–1546.
Seelig, J., Macdonald, P. M., & Scherer, P. G. (1987) *Biochemistry 26*, 7535–7541.
Soltys, C. E., Bian, J., & Roberts, M. F. (1993) *Biochemistry 32*, 9545–9552.
Tausk, R. J. M., Karmiggelt, J., Oudshoorn, C., & Overbeek, J. Th. G. (1974a) *Biophys. Chem. 1*, 175–183.
Tausk, R. J. M., Van Esch, J., Karmiggelt, J., Voordouw, G., & Overbeek, J. Th. G. (1974b) *Biophys. Chem. 1*, 184–193.
Turner, J. D., & Rouser, G. (1970) *Anal. Biochem. 38*, 423–426.
Vold, R. L., Waugh, J. S., Klein, M. P., & Phelps, D. E. (1968) *J. Chem. Phys. 48*, 3831–3839.
White, S. P., Scott, D. L., Otwinoski, Z., Gelb, M. H., & Sigler, P. B. (1990) *Science 250*, 1560–1563.